Journal of the European Ceramic Society 16 (1996) 937–943

S0955-2219(96)00008-8
0955-2219/96/$15.00

Mechanical Properties of Alumina–Metal–Zirconia Nano-Micro Hybrid Composites

Ch. Laurent,[a] A. Rousset,[a] P. Bonnefond,[a,b] D. Oquab[b] & B. Lavelle[b]

[a]Laboratoire de Chimie des Matériaux Inorganiques, URA CNRS 1311, Université Paul-Sabatier, 31062 Toulouse Cedex, France
[b]Laboratoire des Matériaux, URA CNRS 445, Institut National Polytechnique de Toulouse (ENSCT), 31077 Toulouse Cedex, France

(Received 24 February 1995; revised version received 14 December 1995; accepted 5 January 1996)

Abstract

Al_2O_3 and Al_2O_3–2 wt% $Fe_{0.8}Cr_{0.2}$ nanocomposite powders were wet-mixed with different ZrO_2 or Y–ZrO_2 powders. The influence of the ball-milling medium and mixing duration on the microstructure and the amount of tetragonal zirconia retained after hot-pressing are discussed. The fracture strength and fracture toughness of the alumina–metal–zirconia specimens are lower than that of the alumina–metal and alumina–zirconia composites. This could result from a partial annihilation of the different reinforcement mechanisms involved and also from interactions between zirconia and the metallic phase. There is no correlation between the mechanical properties and the amount of tetragonal zirconia. However, the amount of tetragonal to monoclinic transformation at the surface of the specimens during grinding prior to the mechanical tests seems to be a key parameter. © *1996 Elsevier Science Limited.*

1 Introduction

Nanocomposites consisting of nanometric metal particles dispersed within the grains of an alumina matrix have been found to exhibit higher strength and higher toughness than alumina,[1–6] even with a metal content as low as 2 wt% (so about 1 vol%).[2] Although this is not fully understood yet, it seems probable that plastic stretching of the ductile particles,[7] and crack deflection are the main reinforcement mechanisms.

A more popular way to improve the mechanical properties of alumina is based on the dispersion of micrometric zirconia grains as a discrete second phase; zirconia-toughened alumina (ZTA) ceramics have been widely studied (see Wang and Stevens[8] for a review), and several reinforcement mechanisms have been identified, including stress-induced (tetragonal to monoclinic, t → m) phase transformation toughening, microcrack toughening, compressive surface stresses and crack deflection. The combination of these mechanisms is related to the microstructure of the ZTA material, and notably to the extent of agglomeration of the zirconia particles.[8]

Niihara *et al.*[9] have shown that the hybridization of microcomposites and nanocomposites could result in a further improvement in both the strength and toughness. Thus, the aim of this work was to study the mechanical properties of a composite containing both intragranular metal nanoparticles and micrometric zirconia-based particles located in the grain boundaries of alumina.

Results reported in the literature[10–19] on the elaboration of ZTA by mechanical mixing greatly differ regarding the influence of elaboration parameters, such as the ball-milling duration and the nature of the dispersion medium, on the mechanical properties. The first part of this paper deals with the preparation of the alumina–metal–zirconia composite by wet-mixing an Al_2O_3–2 wt% $Fe_{0.8}Cr_{0.2}$ nanocomposite powder prepared in this laboratory with a commercial ZrO_2 powder. $Fe_{0.8}Cr_{0.2}$ is a notation for metal particles containing 80 at% of iron and 20 at% of chromium.

2 Experimental

Details for the synthesis of nanocomposite powders were given in a previous study.[20] Briefly, a solid solution between the requested amounts of the rhomboedral sesquioxides Al_2O_3, Fe_2O_3 and Cr_2O_3 was prepared from the decomposition and

calcination of an oxalate precursor. Pure α-Al_2O_3 was also prepared by the same method. Hydrogen reduction at 1050°C of the solid solution gave rise to the Al_2O_3–2 wt% $Fe_{0.8}Cr_{0.2}$ nanocomposite powder.

A commercial zirconia powder (CERAC Z-1042, monoclinic, average size 10·6 μm, minimum size 0·2 μm, maximum size 20 μm) was mixed and sonicated for 30 min with the nanocomposite powder (average size 2 μm, minimum size 0·2 μm, maximum size 10 μm) in different media: 'acid' water (pH = 5), 'basic' water (pH = 8) and ethanol. The powder/liquid volume ratio was fixed to 50/50 to reduce the risk of differential sedimentation.[19] This was followed by ball-milling, using zirconia balls and vessel, for different times (10, 60 and 360 min). The zirconia content was fixed to 13 wt%. In some cases the Z-1042 powder was dry ball-milled for 60 min prior to sonication ('preground' zirconia). The powders were oven-dried (80°C) and their average size (in volume) was measured using sedimentation granulometry in isopropanol. Transmission electron microscopy (TEM) was also performed to investigate the microstructure. The powders for TEM examination were sonicated in ethanol and a drop of the dispersion was deposited on to a copper grid coated with a collodion film.

The powders were uniaxially hot-pressed in graphite dies at 1450°C under vacuum. The dense specimens (20 mm in diameter and 1 mm thick) were ground successively to 45 and 6 μm with diamond suspensions and a final polish was carried out using 'colloidal' silica (0·05 μm). Relative densities were calculated from the mass and dimensions of the dense composites and found to be equal to or higher than 99%.

Phase identification was performed with X-ray diffraction (XRD) patterns analysis (CoKα = 0·17902 nm) on unground (U), 45 μm-ground (G) and silica-polished (P) specimens. The relative amounts of tetragonal and monoclinic zirconia were calculated from the XRD patterns using the well-known Garvie–Nicholson equation.[21] P specimens were also observed by scanning electron microscopy (SEM). Thin foils for TEM observations were prepared by mechanical grinding and Ar ion-milling.

After a set of preparation parameters has been chosen, mechanical tests were conducted on G specimens. The transverse fracture strength (σ_f) was determined by the three-point-bending test on parallelepipedic specimens (1·6 × 1·6 × 18 mm^3) machined with a diamond saw. The fracture toughness (K_{Ic}) was measured by the SENB method on similar specimens notched using a diamond wire 0·1 mm in diameter. The calibration factor proposed by Brown and Srawley[22] was used to calculate the SENB toughness from the experimental results. Cross-head speed was fixed at 0·1 mm/min. The values given for σ_f and K_{Ic} are the average of measures on seven and six specimens respectively.

Several other zirconia-based powders have been used for these tests: a commercial ZrO_2–5·3 mol% Y_2O_3 powder (CERAC Z-1065, cubic, average size 7·0 μm, minimum size 0·3 μm, maximum size 20 μm), and four products prepared in this laboratory by hydrolysis of $ZrCl_4$ (and YCl_3) aqueous solutions:[23] ZrO_2 (tetragonal) calcined at 500 and 800°C and ZrO_2–2 mol% Y_2O_3 (tetragonal) calcined at 500 and 800°C. The average size of these four powders was about 5·5 μm (minimum size 0·2 μm, maximum size 20 μm), but crystallinity was improved in those calcined at 800°C. A specimen containing only 6·5 wt% of Z-1042 zirconia was also tested.

Table 1 summarizes the characteristics of the zirconia-based powders and gives a letter code for the designation of specimens prepared with these powders.

3 Results and Discussion

3.1 Preparation

The microstructure of the Al_2O_3–2 wt% $Fe_{0.8}Cr_{0.2}$ nanocomposite powder prior to mixing with zirconia is shown in Fig. 1(a). Most of the metal particles are homogeneously dispersed within the alumina grains and are smaller than 3 nm in size. Some larger (5–10 nm) metal particles are located in the pores of the matrix. It has been shown in a previous study[24] that both the alumina grains and the

Table 1. Composition, designation, structure, and average size (as determined by sedimentation granulometry) of the zirconia-based powders

Composition	*Designation*	*Structure*	*Average size (μm)*
ZrO_2(Z-1042)	A13 or A6·5	Monoclinic	10·6
ZrO_2–5·3 mol% Y_2O_3	B	Cubic	7·0
ZrO_2(500°C)	C	Tetragonal	5·5
ZrO_2(800°C)	D	Tetragonal	5·5
ZrO_2–2 mol% Y_2O_3(500°C)	E	Tetragonal	5·4
ZrO_2–2 mol% Y_2O_3(800°C)	F	Tetragonal	5·5

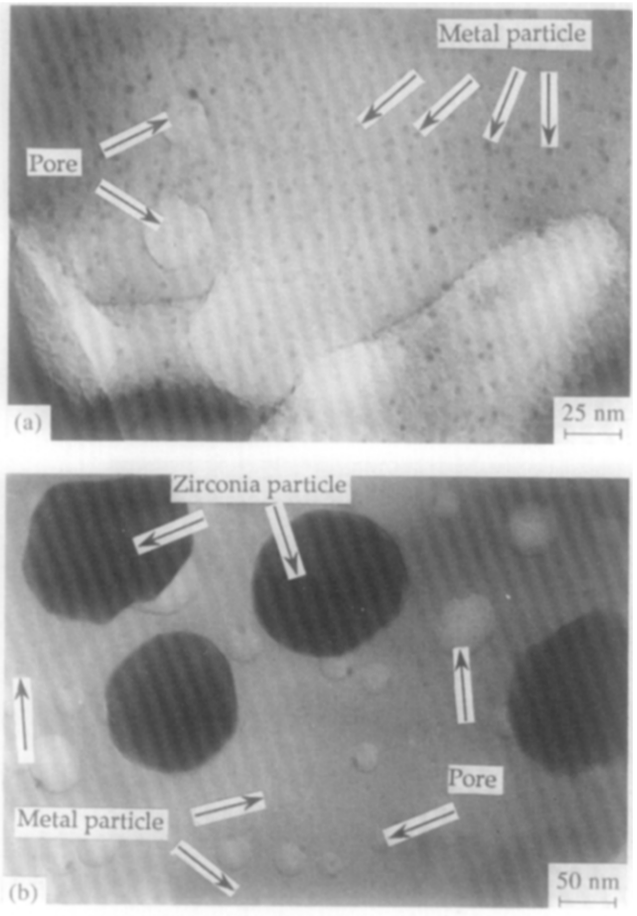

Fig. 1. TEM micrographs showing the microstructure of the Al_2O_3–2 wt% $Fe_{0.8}Cr_{0.2}$ nanocomposite powder (a) and of the alumina–metal–zirconia powder after 60 min ball-milling (b). Some metal particles, pores and zirconia particles are indicated by arrows.

metal particles are monocrystalline and that the intragranular particles are epitaxied in the alumina matrix. The alloy particles are in the stable α form.[20] A TEM micrograph of the alumina–metal–zirconia powder is presented (Fig. 1(b)): it can be seen that metallic dispersion was not affected by the 60 min ball-milling and that 100–150 nm large zirconia particles are located at the surface of the nanocomposite powder grains. The decrease of the powder grain size with the increase in ball-milling duration will be described later in this paper.

The dense composites microstructure as observed by SEM is the same, irrespective of the dispersion medium used: for 10 min ball-milling (Fig. 2(a, b)) there is an inhomogeneous distribution of zirconia agglomerates, the size of which ranges from a few micrometers to 60 μm. As expected, a more even distribution is achieved with the increase in ball-milling time to 60 min, the size of the zirconia agglomerates being lower than 10 μm (Fig. 2(c, d)). Ball-milling for 360 min only results in a slight re-agglomeration of the zirconia particles (Fig. 2(e,f)).

XRD patterns analysis revealed the presence of α-Al_2O_3, t-ZrO_2, m-ZrO_2 and α-$Fe_{0.8}Cr_{0.2}$. The {110} metal peak is very weak and the calculation of the average size of the metal particles using Scherrer's method is not possible. Since a high content of tetragonal zirconia is known to be beneficial with respect to the mechanical properties, we have plotted the t-ZrO_2 content as deduced from XRD measurements on unground (U) specimens versus the average size of the composite powder (Fig. 3). Ball-milling the starting powders for 10, 60 and 360 min reduces the average grain size to about 3, 2 and 1·5 μm respectively; the size distribution is also reduced (maximum size lower than 7 μm after 60 and 360 min ball-milling). However, this has no influence on the amount of tetragonal zirconia retained after hot-pressing, since the higher measured value is equal to 30% and all values are within the 14–30% range. The data presented in Fig. 3 also show little difference between the dispersion media, but more t-ZrO_2 is generally obtained using 'pre-ground' zirconia. Thus, it appears that whatever the elaboration process, agglomeration of the zirconia particles in our dense materials is strong enough to allow a majority of particles to undergo the spontaneous (t $\rightarrow$ m) phase transformation during cooling from the hot-pressing temperature.

Due to the development of high stresses during grinding, which favour the tetragonal-to-monoclinic (t $\rightarrow$ m) phase transformation, the t-ZrO_2 content is found to be markedly lower in G specimens (ranging between 12 and 26%). The values measured in P specimens are very close to that in U specimens, showing that P values are representative of the bulk t-ZrO_2 content and that the lower G values are only due to grinding. The compressive stresses that develop at the surface of the material owing to the volume increase associated with the (t $\rightarrow$ m) transformation are known to be beneficial with respect to fracture strength.[25] Thus, to quantify the grinding-induced (t $\rightarrow$ m) phase transformation we have defined R as the ratio of the t-ZrO_2 content in G specimens to the t-ZrO_2 content in U specimens. R is not dependent on the ball-milling time (for example R = 0·88, 0·88 and 0·86 for 10, 60 and 360 min mixing in ethanol respectively); however R is equal to about 0·76 when 'pre-ground' zirconia was used, except in 'basic' water in which values close to 0·87 are still measured. This could indicate that higher stresses would be necessary to further transform the t-ZrO_2 particles in specimens prepared in this medium.

According to this preliminary study, the following set of preparation parameters has been chosen: 'pre-grinding' of the zirconia-based powder, mixing with the nanocomposite powder in 'basic' (pH = 8) water (30 min sonication followed by 60 min ball-milling), and oven-drying.

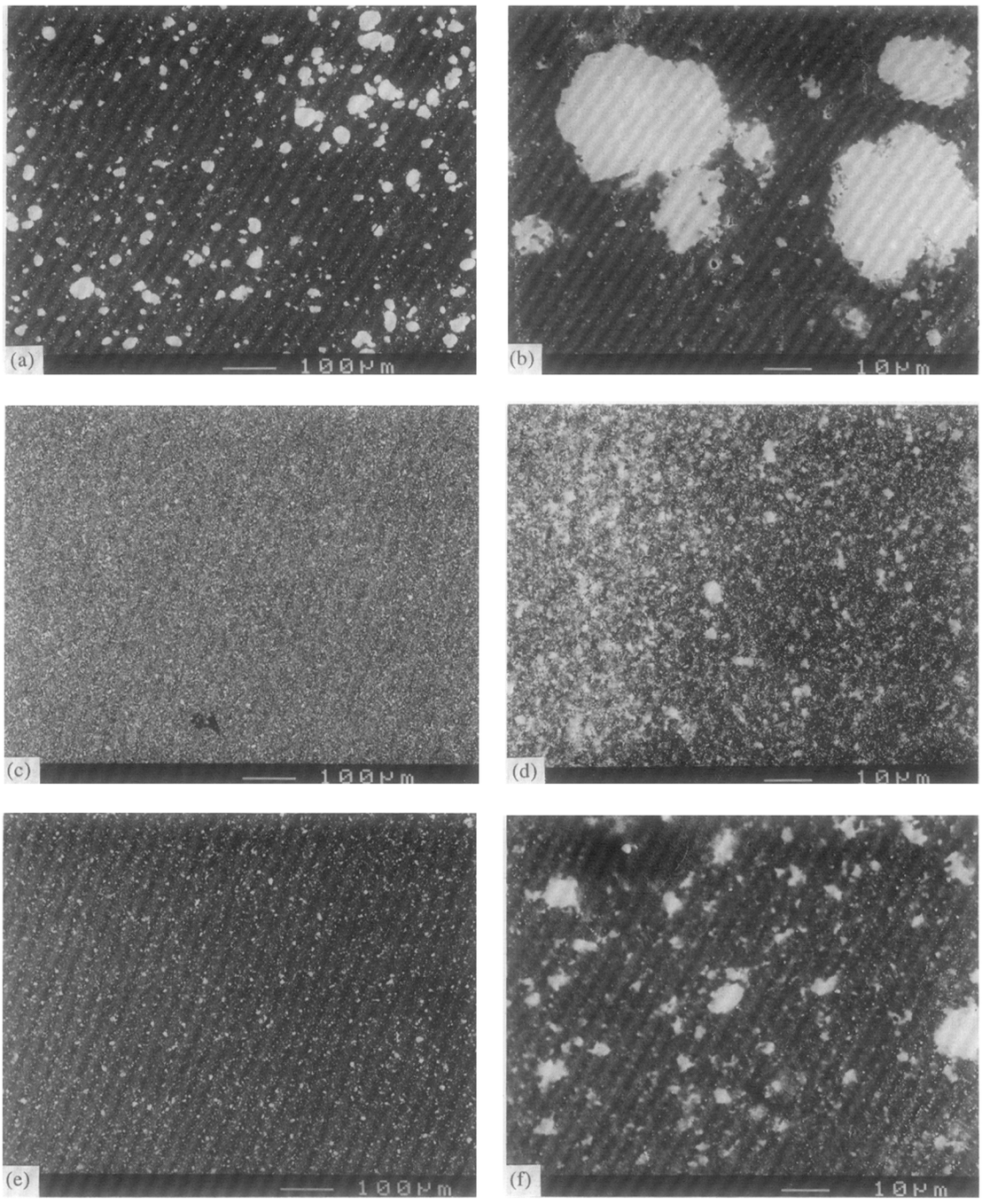

Fig. 2. SEM micrographs showing the microstructure of silica-polished (P) specimens after 10 min ((a),(b)), 60 min ((c),(d)) and 360 min ((e),(f)) ball-milling (the dispersion medium was found to have no or very little influence).

A TEM micrograph of the A13 composite prepared according to this process and hot-pressed in vacuum at 1450°C is shown in Fig. 4. The zirconia particles are mainly located at the grain boundaries and triple grain junctions of the alumina matrix. The shape of some is elongated because their formation results from agglomeration of several particles (see the particle in the upper right hand corner of Fig. 4). The alumina grains are micrometric in size (1 μm for this particular grain, but in fact closer to 2 μm) and seem to be quite porous, but some of the larger holes probably correspond to the location of zirconia particles entrapped in the alumina grain that were extracted during ion-milling; accordingly, some of the smaller holes could correspond to the location of nanometric metal particles. Some metal particles smaller than 20 nm can be seen on Fig. 4.

3.2 Mechanical properties

In order to discriminate the effects on mechanical properties of zirconia on the one hand and of metal nanoparticles on the other hand, an alumina–zirconia (Z-1042) specimen (denoted H hereafter) was also prepared. The t-ZrO_2 content measured in G specimens, R ratio, and results of the mechanical tests, including those previously published[2] of the Al_2O_3–2 wt% $Fe_{0.8}Cr_{0.2}$ nanocomposite

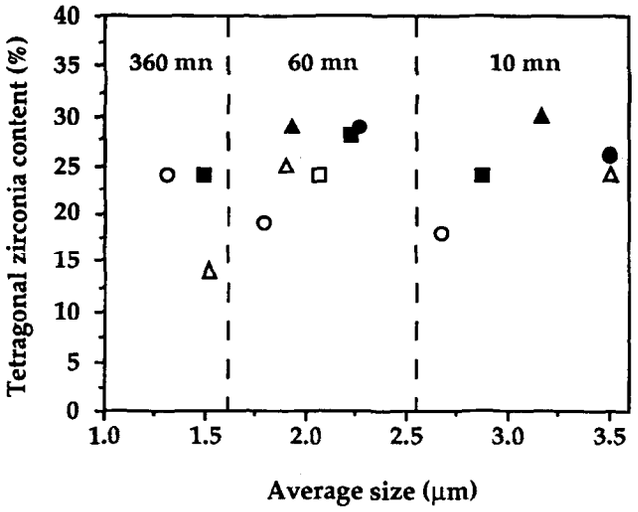

Fig. 3. Amount of tetragonal zirconia in unground (U) specimens versus the average size of the composite powder as determined by sedimentation granulometry. Full symbols denote dry ball-milling of the zirconia powder before sonication. Circle: water (pH = 5); square: water (pH = 8); triangle: ethanol. Ball-milling duration is indicated.

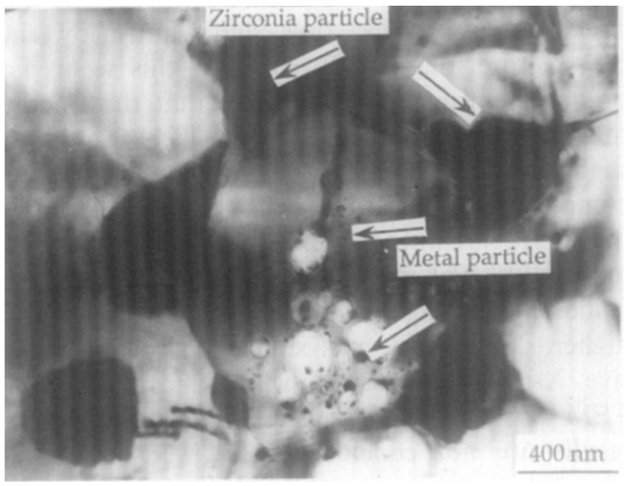

Fig. 4. TEM micrograph of the A13 alumina–metal–zirconia dense composite. Some metal particles and zirconia particles are indicated by arrows.

(denoted N hereafter) and alumina, are listed in Table 2. The size of the alumina grains in these latter composites is close to 2 μm and thus similar to that found in the alumina–metal–zirconia specimens.

It should be noted that the amount of tetragonal zirconia is fairly low, even when using tetragonal zirconia starting powders (C, D, E, F). However, the t-ZrO_2 content is much higher (34 and 51% in G and U specimens respectively) when a lower amount of zirconia is dispersed in alumina (A6·5). These results confirm that our preparation method does not allow the zirconia particles to disperse homogeneously enough at the surface of the nanocomposite to prevent agglomeration during hot-pressing. The minimum value of R is 0·67 (in A6·5) and the maximum is 1, i.e. no transformation (in E). The trend is that R decreases with the increase in t-ZrO_2, which seems to indicate that a higher proportion of these particles would also be available to undergo the (t $\rightarrow$ m) phase transformation during grinding. However, this is not strictly followed, due probably to the microstructural and compositional differences that exist between our composites.

The mechanical properties of the alumina–zirconia composite (H, σ_f = 712 MPa and K_{Ic} = 5·4 MPa$\sqrt{m}$), as well as those achieved using cubic zirconia (B, σ_f = 590 MPa and K_{Ic} = 4·5 MPa$\sqrt{m}$), which is known to not promote the mechanical reinforcement,[26] are similar to that found in the literature.[8,26] In particular, it should be noted that the fracture strength of the alumina–zirconia composite (H) is of the order of that of the metal-alumina nanocomposite (N), showing the validity of our wet-mixing preparation method with respect to preparing composite material with reasonably high strength and toughness.

Concerning the hybrid composites, all fracture strength values are lower than that of the reference materials (H and N), and all K_{Ic} values are lower than that of the nanocomposite. The fracture strength of specimen A6·5, which contains a higher amount of tetragonal zirconia, is higher than that of A13, but there is otherwise no correlation between the mechanical properties and the t-ZrO_2 content.

Table 2. Fracture strength, fracture toughness, tetragonal zirconia content (G specimens), and R ratio (see text). Values for Al_2O_3 and N are from Reference 2. Standard deviation on σ_f and K_{Ic} values is indicated between brackets

Specimen	σ_f *(MPa)*	K_{Ic} *(Mpa*$\sqrt{m}$*)*	*t-ZrO_2 content (%)*	*R*
Al_2O_3	335 (20)	4·4 (0·3)	—	—
N	690 (127)	6·5 (0·2)	—	—
H	712 (40)	5·4 (0·4)	16	0·70
A6·5	620 (124)	5·5 (1·0)	34	0·67
A13	572 (40)	5·7 (0·4)	22	0·82
B	590 (62)	4·5 (0·3)	100% cubic	—
C	510 (28)	5·2 (0·6)	22	0·88
D	612 (16)	5·6 (0·5)	19	0·79
E	486 (36)	5·0 (0·4)	17	1·00
F	582 (31)	6·0 (0·5)	15	0·79

On the contrary, it is interesting to note that both the lower σ_f and K_{Ic} are achieved with specimen E, which do not exhibit (t → m) phase transformation during grinding (R = 1). Plotting fracture strength versus R (Fig. 5(a)) suggests that the higher σ_f is obtained for an optimal value of R (about 0·74). A similar evolution is observed for K_{Ic} (Fig. 5(b)). This could represent an optimal combination of stress-induced (t → m) transformation toughening and compressive surface stresses, the microcrack toughening mechanism being roughly of the same importance in all specimen, which contain a similar amount of monoclinic zirconia.

R could also be related to the transformation zone depth whose influence is discussed by Kosmac *et al.*[27] Our results are in qualitative agreement with theirs, since they have shown that the higher toughness is not obtained for the larger transformation zone depth, but for a particular combination of several factors: zone depth, t-ZrO_2 content and size of the zirconia particles.

Obviously, the additive effect that was expected from the hybridization of nano- and microcomposites is not observed. The lower mechanical properties achieved with the alumina–metal–zirconia composites could result from a partial annihilation of the different reinforcement mechanisms: indeed, SEM observations (Fig. 6) show that the fracture is mostly intergranular, while it is essentially

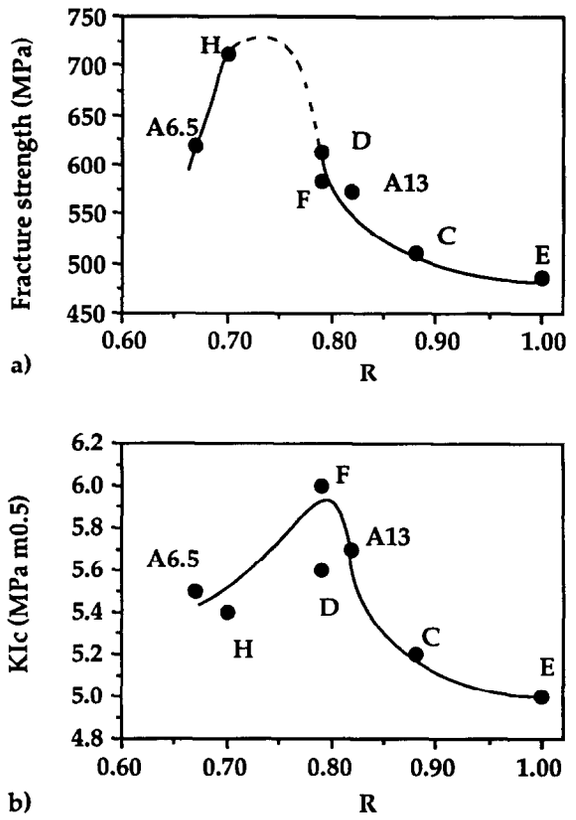

Fig. 5. Fracture strength (a) and fracture toughness (b) versus R ratio (see text). Dashed part of the curve is only speculative.

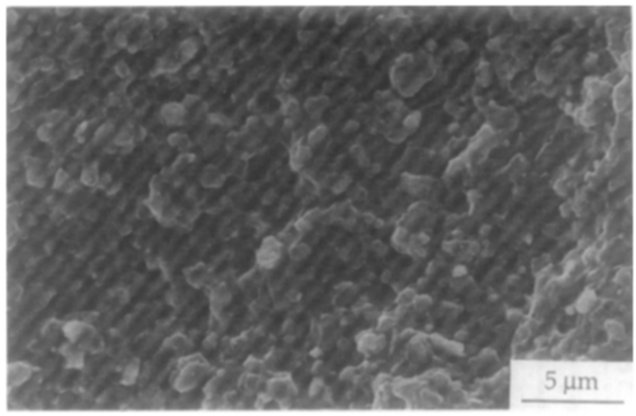

Fig. 6. SEM micrograph showing the fracture surface of an alumina–metal–zirconia composite.

intragranular in the absence of zirconia.[28] Thus, mechanisms involving the metal particles, which are located within the matrix grains, would be far less operative. On the other hand, the metal nanoparticles could favour the coalescence of the residual microcracks due to the (t → m) transformation taking place during cooling from the hot-pressing temperature, thus significantly lowering the fracture toughness.[8] However, this seems not probable since one can observe that the fracture toughness of specimens A6·5, A13, D and F is slightly higher than that of the alumina–zirconia composite (H). The diffusion at high temperatures of Fe species into zirconia, which is known[29] to increase the volume difference between the monoclinic and tetragonal phases, could provoke a higher, detrimental, microcracking. Energy dispersive X-ray spectroscopy was performed during TEM observations to check this point, but the results are not conclusive. However, Tuan and Chen[30,31] recently reported that interactions between micrometric silver and zirconia particles do not favour the additive effect.

4 Conclusions

'Nano-micro hybrid composites' have been prepared by wet-mixing and hot-pressing a zirconia powder and a 2 wt% metal–alumina nanocomposite powder. The nanometric metal particles are dispersed within the matrix grains and the zirconia particles are located at the grain boundaries of alumina. Owing to the agglomeration of zirconia particles, the amount of tetragonal zirconia is fairly low (≤ 30%) even when using t-ZrO_2 starting powders; however, it was observed to increase when using a lesser amount of zirconia. The validity of the chosen elaboration method (60 min ball-milling in pH 8 water) is demonstrated by the mechanical properties achieved with the 13 wt%

zirconia–alumina composite (without metal): σ_f = 712 MPa and K_{Ic} = 5·4 MPa$\sqrt{m}$).

Instead of the expected additive strengthening and toughening effects, annihilation of the reinforcement mechanisms occurs in the hybrid composites. Explanations for this may be found in the microstructure of the material and also in interactions between zirconia and the metallic phase. The amount of tetragonal to monoclinic transformation at the surface of the specimens during grinding prior to the mechanical tests was identified to be a key parameter, showing the importance of the effect of compressive surface stresses in these materials.

References

1. Devaux, X., Laurent, Ch., Brieu, M. & Rousset, A., Propriétés microstructurales et mécaniques de nanocomposites à matrice céramique. *C. R. Acad. Sci. Paris*, **312** Série II (1991) 1425–30.
2. Devaux, X., Laurent, Ch., Brieu, M. & Rousset, A., Ceramic matrix nanocomposites. In *Composites Materials*, eds A. T. Di Benedetto, L. Nicolais & R. Watanabe. Elsevier Science Publishers B. V., Amsterdam, 1992, pp. 209–14.
3. Laurent, Ch., Devaux, X., Brieu, M. & Rousset, A., Microstructural and mechanical properties of alumina–iron–chromium alloys nanocomposites. In *Euro-Ceramics II*, eds G. Ziegler & H. Hausner. Deutsche Keramische Gesellschaft e. V., Köln, 1992, pp. 1679–83.
4. Breval, E., Deng, Z., Chiou, S. & Pantano, C. G., Sol–gel prepared Ni–alumina composite materials. Part I. Microstructure and mechanical properties. *J. Mat. Sci.*, **27** (1992) 1464–8.
5. Sekino, T., Nakahira, A., Niihara, K. & Nawa, M., Fabrication of Al_2O_3/W nanocomposites. *KONA Powder and Particle*, **10** (1992) 192–7.
6. Sekino, T., Nakahira, A., Nawa, M. & Niihara, K., Fabrication and mechanical properties of tungsten metal dispersed Al_2O_3 based nanocomposites. In *Proceedings of the International Conference Ceramics adding the Value:Austceram 92*, ed. M. J. Bannister, CSIRO, Australia, 1992, pp. 745–50.
7. Evans, A. G., High toughness ceramics. *Mat. Sci. Eng. A*, **105–106** (1988) 65–75.
8. Wang, J. & Stevens, R., Review. Zirconia-toughened alumina (ZTA) ceramics. *J. Mat. Sci.*, **24** (1989) 3421–40.
9. Niihara, K., Nakahira, A. & Sekino, T., New nanocomposite structural ceramics. *Mat. Res. Soc. Symp. Proc.*, **286** (1993) 405–12.
10. Brodhag, C., Bach, J. P., Thevenot, F. & Deletter, M., Microstructure of zirconia-toughened alumina obtained through different precursor routes. *Mat. Sci. Eng. A*, **109** (1989) 53–9.
11. Tomaszewski, H. & Kulczycki, A., Effect of Y_2O_3 partial stabilization on thermomechanical properties of Al_2O_3–ZrO_2 ceramic. In *Advanced Structural Inorganic Composites*, ed. P. Vincenzini, Elsevier Sci. Pub. B. V., Amsterdam, 1991, pp. 391–400.
12. Samdi, A., Grollier-Baron, Th., Roubin, M. & Durand, B., Etude des conditions de dispersion optimale de poudres de zircone obtenues par pyrolyse d'acétates de zirconium. *Powder Tech*, **66** (1991) 237–42.
13. Yoshimatsu, H., Miura, Y., Osaka, A., Kawasaki, H. & Omori, S., Mechanical properties of zirconia–alumina composite ceramics prepared from Zr–Al organometallic compounds. *J. Mat. Sci.*, **25** (1990) 5231–6.
14. Hoshi, Y., Obitu, M., Awano, M. & Takagi, H., Al_2O_3–PSZ ceramics with high flexural strength and high fracture toughness. *Interceram*, **32** (1990) 84–7.
15. Homerin, P., Thévenot, F., Orange, G., Fantozzi, G., Vandeneede, V., Leriche, A. & Cambier, F., Mechanical properties of zirconia toughened alumina prepared by different methods. *J. Phys.*, C1, **47** (1986) 717–21.
16. Carlstrom E. & Lange F. F., Mixing of flocced suspensions. *J. Am. Ceram. Soc.*, **67** (1984) C-169–70.
17. Bleier, A. & Westmoreland, G., Chemical and physical principles of processing that effect microstructure of Al_2O_3–ZrO_2 composites. *Mat. Res. Soc. Symp. Proc.*, **121** (1988) 145–54.
18. Leuwerink, T. H. P., Den Exter, P., Winnubst, A. J. A. & Burggraaf, A. J., Characteristics of wet chemically prepared zirconia/alumina ceramics. In *Advanced Structural Inorganic Composites*, ed. P. Vincenzini, Elsevier Sci. Pub. B. V., Amsterdam, 1991, pp. 619–28.
19. Glennie, D. & Konsztowicz, K. J., Homogenization of dense acqueous suspensions of ZTA composites. In *Advanced Structural Inorganic Composites*, ed. P. Vincenzini, Elsevier Science Publishers BV, Amsterdam, 1991, 629-36.
20. Devaux, X., Laurent, Ch. & Rousset A., Chemical synthesis of metal nanoparticles dispersed in alumina. *Nanostruct. Mater.*, **2** (1993) 339–46.
21. Garvie, C. & Nicholson, P. S., Phase analysis in zirconia systems. *J. Am. Ceram. Soc.*, **55** (1972) 303–5.
22. Brown, W. F. & Srawley, J. E., *Plane Strain Crack Toughness Testing of High Strength Metallic Materials.* ASTM Spec. Tech. Pub., 410, ASTM, Philadelphia, PA, USA, 1966.
23. Haberko, K., Characteristics and sintering behaviour of zirconia ultrafine powders. *Ceramurgia International*, **5** (1979) 148–53.
24. Devaux, X., Laurent, Ch., Brieu, M. & Rousset, A., Iron–alumina interface in ceramic matrix nanocomposites. *J. All. Comp.*, **188** (1992) 179–81.
25. Lange, F. F., Transformation toughening. Part 4. Fabrication, fracture toughness and strength of Al_2O_3–ZrO_2 composites. *J. Mat Sci.*, **17** (1982) 247–54.
26. French, J. D., Chan, H. M., Harmer, M. P. & Miller, G. A., Mechanical properties of interpenetrating microstructures: the Al_2O_3/c-ZrO_2 system. *J. Am. Ceram. Soc.*, **75** (1992) 418–23.
27. Kosmac, T., Swain, M. V. & Claussen, N., The role of tetragonal and monoclinic ZrO_2 particles in the fracture toughness of Al_2O_3–ZrO_2 composites. *Mat. Sci. Eng.*, **71** (1985) 57–64.
28. Laurent Ch., Contribution à l'étude de nanocomposites à matrice céramique. Alumine - alliages fer–chrome et alumine–zircone–fer et alliages fer–chrome. Doctoral Thesis, Université Paul-Sabatier, Toulouse, France, 1994.
29. Beck, H. P. & Kaliba, C., On the solubility of Fe, Cr and Nb in ZrO_2 and its effects on the thermal dilatation and polymorphic transitions. *Mater. Res. Bull.*, **25** (1990) 1161–8.
30. Tuan, W. H. & Chen, W. R., Enhancing the mechanical performance of alumina through the addition of metallic and ceramic inclusions. In *Third Euro-Ceramics* Vol. 3, eds P. Duran & J. F. Fernandez, Faenza Editrice Iberica S. L., 1993, pp. 713–18.
31. Tuan, W. H. & Chen, W. R., The interactions between silver and zirconia inclusions and their effect on the toughening behaviour of Al_2O_3/(Ag + ZrO_2) composites. *J. Eur. Ceram. Soc.*, **14** (1994) 37–43.